Inorganic Chemistry

Article

pubs.acs.org/IC

Selective Fluorescence Sensing of Copper(II) and Water via Competing Imine Hydrolysis and Alcohol Oxidation Pathways Sensitive to Water Content in Aqueous Acetonitrile Mixtures

Kadarkaraisamy Mariappan, Madhubabu Alaparthi, Gerald Caple, Vinothini Balasubramanian, Mariah M. Hoffman, Mikaela Hudspeth, and Andrew G. Sykes*

The Department of Chemistry, University of South Dakota, Vermillion, South Dakota 57069, United States

Supporting Information

ABSTRACT: Addition of hydrazines to a 1,8-disubstituted anthraquinone macrocycle containing a polyether ring produces site-selective imination, where hydrazone formation produces the more sterically hindered adduct. Reduction of the remaining carbonyl group to a secondary alcohol followed by addition of copper(II) ion causes intense yellow fluorescence to occur, which is selective for this metal cation and allows this system to be used as a fluorescence sensor. In the presence of water, a green-fluorescent intermediate appears, which slowly decomposes to produce the original starting anthraquinone. The addition of a large amount of water radically changes the reaction pathway. In this case, oxidation of the secondary alcohol is kinetically faster than hydrolysis of the hydrazone, although the same anthraquinone product is ultimately produced. Stern−Volmer data suggest that dioxygen quenches the green emission through both dynamic and static mechanisms; the static ground-state effect is most likely due to association of oxygen with the copper-bound fluorescent intermediate.

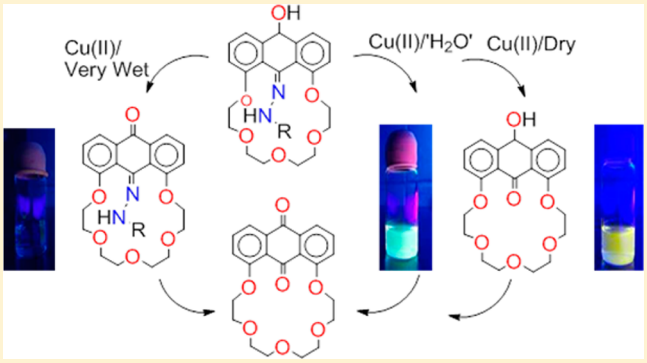

INTRODUCTION

The selective detection of metals is of particular importance to the fields of environmental chemistry and biochemistry. Detection of copper(II) is of particular interest as it is an essential metal in all living organisms because of its catalytic and oxidative properties.[1] Copper is the third most abundant transition metal in the human body, with only iron and zinc being higher in concentration.[2] Unregulated Cu(II) can cause oxidative stress and has been shown to have connections to aging and such neurodegenerative diseases as Menke's, Wilson's, amytrophic lateral sclerosis, Alzheimer's, prion, and Parkinson's diseases.[1,3]

The amount of biologically available copper has increased as a result of anthropogenic activities such as smelting, mining, fertilizing, and the use of fungicides and molluscicides.[4] Increased copper levels have proven to be detrimental to the growth of certain vegetation,[5] stream insects,[6] aquatic biota, and microbes, among others.[4]Because of the toxicity of Cu(II), the United States Environmental Protection Agency's maximum contaminant level goal for Cu(II) in drinking water is 1.3 mg/L (~1 ppm).[7]Detection of Cu(II) is critical for the identification of polluted bodies of water and regulation of human drinking water, and this ion has typically been detected in the past by atomic absorbance spectroscopy, inductively coupled plasma, voltammetry, and piezoelectric quartz crystals, which are often expensive and time-consuming methods.[8] An alternative method for selective detection is the use of fluorescence spectroscopy. Fluorescent sensors are advantageous because they are often inexpensive, convenient, selective, and sensitive.[8,9] While numerous copper sensors have been reported, many of these are fluorescence quenching sensors (turn-off sensors) because of the paramagnetic nature of the metal center.[10]In order to maximize spatial resolution, fluorescence enhancement sensors (turn-on sensors) are generally preferred over turn-off sensors.[1] Cu(II) sensors with turn-on fluorescence can be categorized primarily into photoinduced electron transfer (PET)-type,[11] rhodamine spirolactam ring-opening-type,[12] and internal charge transfer (ICT)-type[13] sensors. Other Cu(II) detection mechanisms have included copper-catalyzed coupling reactions[14] and the use of nanoparticles.[15]

We recently reported a series of imines **2** based on site-selective imination of the external carbonyl of quinone macrocycle **1** (Scheme 1) using Ti(IV) as a catalyst.[16] Reduction with $NaBH_4$ yields alcohol **3**, which undergoes imine−enamine tautomerization, resulting in turn-on fluorescence, only in the presence of Zn(II).[17] Very few analyte-specific fluorescence sensor systems currently employ tautomerization as the operating photophysical mechanism. Surpris-

Received: October 31, 2013
Published: March 6, 2014

   dx.doi.org/10.1021/ic402723c | *Inorg. Chem.* 2014, 53, 2953−2962

Scheme 1. Site-Selective Syntheses of External Imines (2[16] and 3[17]) and Internal Hydrazones (4 and 5, This Work)

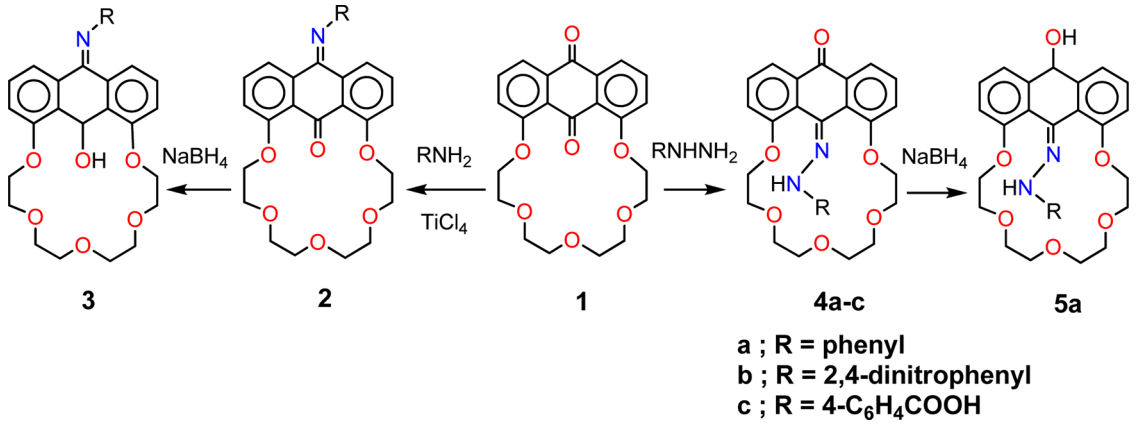

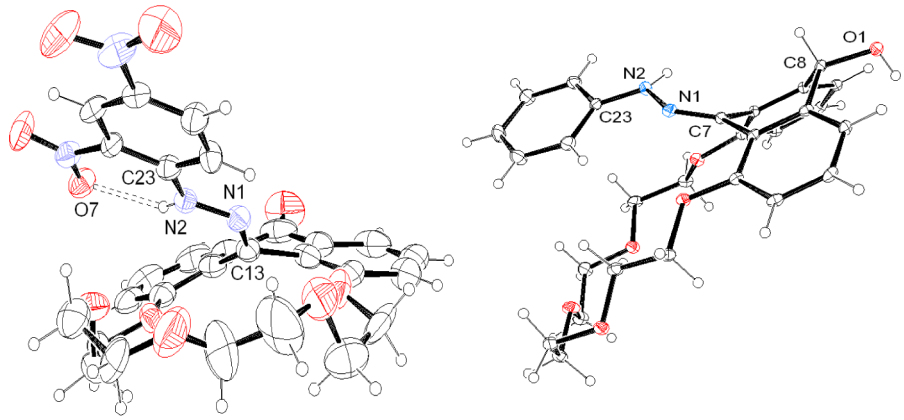

Figure 1. (left) Thermal ellipsoid diagram (293 K, 30%) of **4b**. Imine: C13−N1 = 1.301(7) Å; N1−N2 = 1.341(7) Å. Carbonyl: C34−O11 = 1.216(10) Å. Intramolecular hydrogen bond: N2−O7 = 2.637(7) Å, N2−H···O7 = 137(4)°. (right) Thermal ellipsoid diagram (100 K, 30%) of **5a**·CH_2Cl_2. Imine: C7−N1 = 1.285(4) Å; N1−N2 = 1.376(4) Å. Alcohol: C8−O7 = 1.414(4) Å. The dichloromethane solvate has been removed for clarity.

ingly, we have found that the addition of hydrazines to **1** exclusively yields hydrazones **4** via condensation with the opposing intraannular carbonyl instead. Reduction yields the corresponding alcohol **5**, which undergoes an intense fluorescence enhancement in the presence of Cu(II) that is dependent on the amount of water present in the solvent.

RESULTS

Synthesis. Commercially available aromatic hydrazines condense with **1** in the presence of sulfuric acid to produce bright-orange hydrazones **4**, a familiar reaction typically used for the qualitative identification of carbonyl groups in the introductory organic chemistry laboratory (Scheme 1). Here, however, the reaction is site-selective, condensing only with the intraannular carbonyl group, even when the hydrazine is present in excess. The resonances for the anthraquinone protons remain relatively unchanged from those of the starting compound **1**, indicating that the external carbonyl remains unreacted. X-ray analysis of crystals of **4b**, the 2,4-dinitrophenyl derivative, conclusively showed that the hydrazone formed results from condensation only with the internal carbonyl (Figure 1 left). The bond distances are typical for double bonds for both the imine and carbonyl groups found within the structure. Previously, this compound was incorrectly described in the literature as the external adduct because of the possibility that the crown ring, through steric interactions, would block hydrazone formation at the internal carbonyl,[19] and other prior cyclic crown ethers had previously yielded external azophenolic acerands.[20] However, we have always found that the intraannular carbonyl is the most reactive carbonyl, undergoing a kinetically facile reduction with $NaBH_4$ in the case of **1** alone, likely due to the electronic inductive effect of the nearby alkoxy groups;[21] thus, it is apparent that the "butterfly" motion of the anthraquinone backbone is flexible enough to accommodate "internal" hydrazone formation here.

Reduction of **4a** with $NaBH_4$ produces compound **5a**, in which the external carbonyl has been reduced to the corresponding alcohol (Scheme 1). IR data show the loss of the carbonyl stretch and the introduction of a new OH stretch, and the proton NMR spectrum shows the appearance of one methine proton at 5.31 ppm (coupling constant J = 8 Hz) coupled to the OH proton at 6.37 ppm (J = 8 Hz) (Figure S1 in the Supporting Information). In the structure of compound **5a** (crystallized as the CH_2Cl_2 solvate; Figure 1 right), the C═N imine group reflects an unreduced −N═N− double bond (C7−N1 = 1.285 Å) while the carbonyl has been reduced to the alcohol (C8−O1 = 1.414 Å). The N−H and O−H protons in the structure form hydrogen bonds to crown ether oxygen atoms of neighboring molecules. Unlike **4a**, the dinitrophenyl adduct **4b** could not be reduced to the corresponding alcohol using the same reaction conditions.

dx.doi.org/10.1021/ic402723c | Inorg. Chem. 2014, 53, 2953−2962

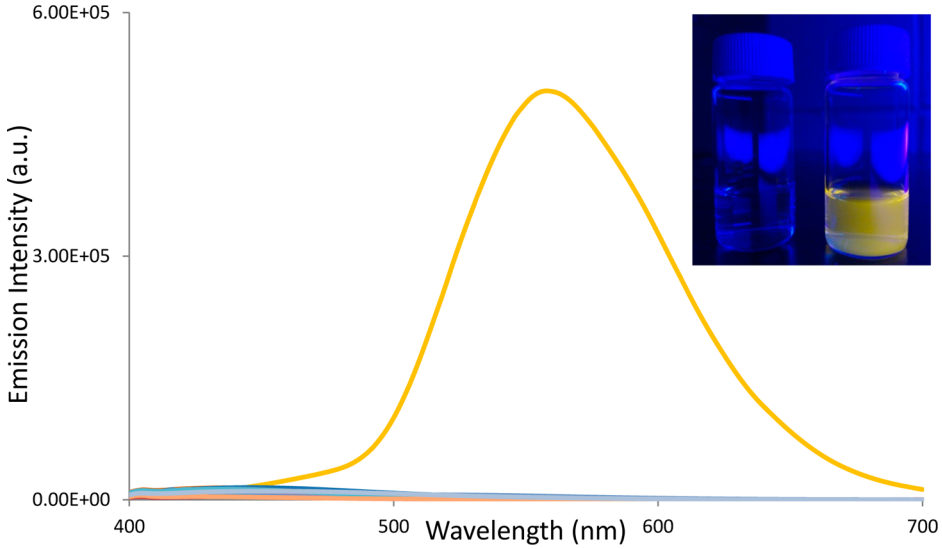

Figure 2. Changes in the fluorescence of **5a** (1.0×10^{-4} M) in acetonitrile upon the immediate addition of 2.0 equiv of metal cations, with excitation at 360 nm. Inset: photograph showing solutions of **5a** under irradiation before and immediately after addition of Cu(II).

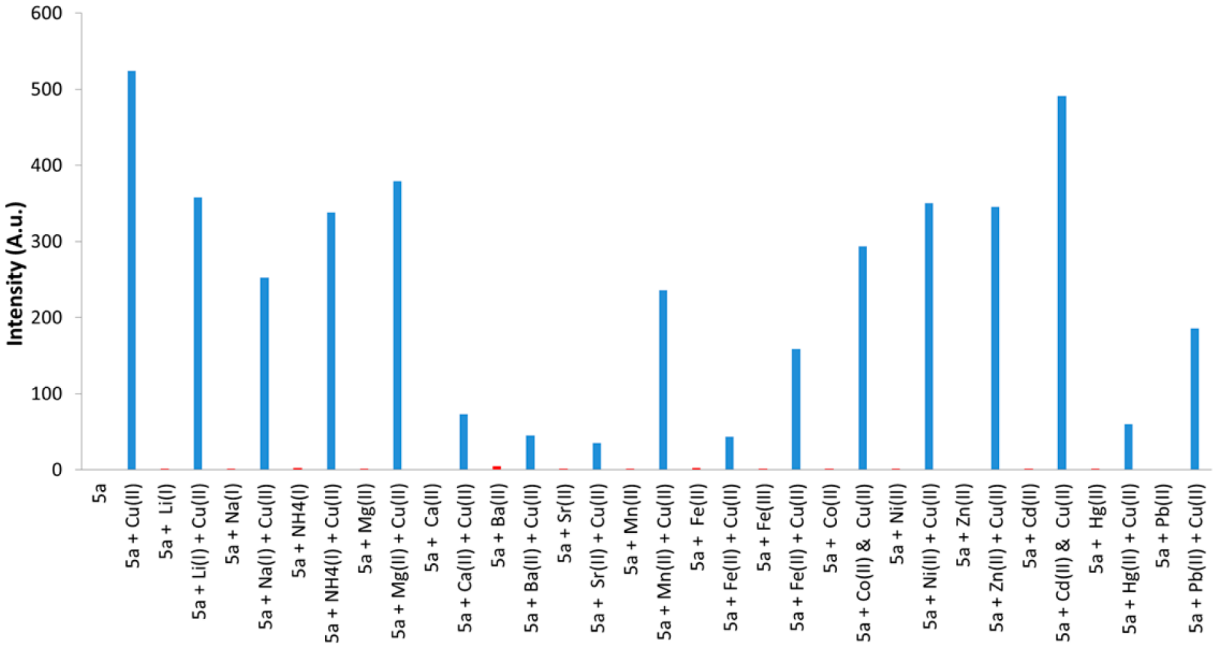

Figure 3. Competition study: addition of two equivalents of selected metal cations to solutions of **5a** (1.0×10^{-4} M). Fluorescence was monitored at 560 nm, and the excitation wavelength was 360 nm. Red and blue bars are before and after addition of Cu(II), respectively.

Spectroscopy. The addition of different metal cations to **5a** in acetonitrile was studied, and it was found that only Cu(II) causes the immediate appearance of an intense yellow emission (Figure 2). The addition of other cations prior to addition of Cu(II) did show competition from the lower alkaline-earth metals and paramagnetic transition-metal cations (Figure 3). We previously demonstrated that oxophilic cations, such as Ca(II) and Pb(II), have the highest affinity for the same crown ether ring size and may block the association of Cu(II) within the macrocycle.[22,23]

Final Product Identification. Under very dry conditions, the yellow emission fades to form a nonemissive solution within a few minutes (Figure 4 left). We identified the final nonemissive product as compound **1**, the original anthraquinone starting material as shown in Scheme 1, indicating that both hydrolysis of the hydrazone and oxidation of the alcohol back to the quinone occur upon the addition of Cu(II). We isolated compound **1** as the final product by means of ^{1}H NMR spectroscopy (Figure S1) and X-ray crystallography (Figure S2). Addition of $CuCl_2$ to **5a** in a 1:1 ratio yields yellow crystals composed of **1**·$CuCl_2$ upon evaporation. The proton NMR spectrum is identical to that of an authentic sample of **1**, and the X-ray structure shows a simple adduct of **1** cocrystallized with $CuCl_2$. Of interest is the fact that the copper metal center remains in the +2 oxidation state with the presence of two chloride anions bound in a linear arrangement around the metal center.

However, when only a small amount of water (0.2−0.3% w/v, ~0.14 M) is present in the solution, the yellow emission is rapidly replaced by an intense green emission at ~490 nm

dx.doi.org/10.1021/ic402723c | Inorg. Chem. 2014, 53, 2953−2962

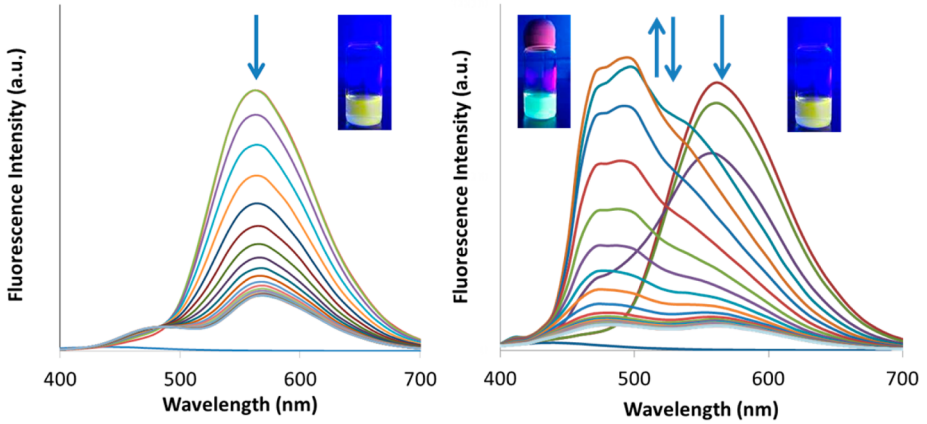

Figure 4. (left) Fluorescence changes after addition of 2.0 equiv of Cu(II) to 1.0×10^{-4} M **5a** in ~1.4×10^{-3} M H_2O in acetonitrile. (right) Fluorescence changes after addition of 2.0 equiv of Cu(II) to 1.0×10^{-4} M of **5a** in ~0.14 M H_2O in acetonitrile. The emission spectra were collected every 15 s, and the excitation wavelength was 360 nm.

Scheme 2. Cu(II)-Catalyzed Oxidation and Hydrolysis of 4a

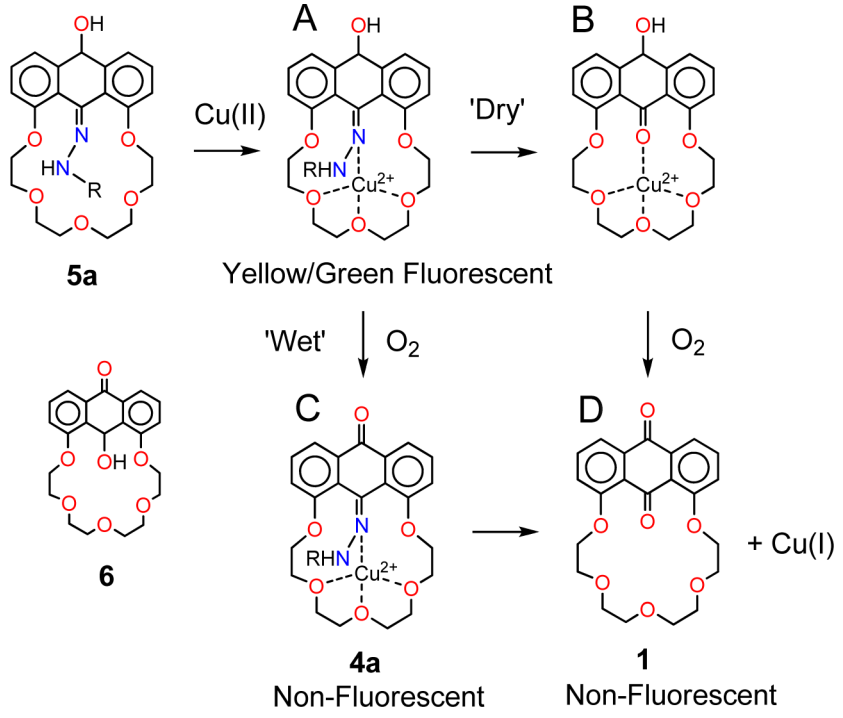

(Figure 4 right). Thus, compound **5a** is not only a sensitive fluorescent copper(II) sensor but also a fluorescent water sensor. The green emission diminishes over a few minutes to yield a nonemissive solution, in which the final product was similarly identified as **1**.

Reaction Mechanism. Scheme 2 represents two possible pathways for the transformation of **5a** to the final nonemissive product **1**. Potentially, either hydrolysis of the hydrazone (**A** → **B**) or oxidation of the alcohol (**A** → **C**) could take place first. Under conditions with little water present (vide infra), we propose that the hydrazone is first hydrolyzed by the Cu(II) ion to form intermediate **B**, which then undergoes oxidation by dissolved oxygen to produce the quinone (**D**).

Evidence for this pathway comes from the UV/vis spectral changes (Figure 5), an ^{1}H NMR titration after addition of Cu(II) (Figure S3), and mass spectrometry data (Figure S4). The absorbance changes upon the addition of Cu(II) to **5a** in 99:1 acetonitrile/water solution (Figure 5) show the appearance of an intermediate band at ~330 nm, which we attribute to the formation of the hydrolyzed intermediate **B**. The intermediate appears immediately upon Cu(II) addition and subsequently reacts to form product **D** with very clean isosbestic points. Intermediate **B** happens to be the isomer of compound **6** (Scheme 2), which we previously isolated and found to be air-stable.[21,24] The absorption spectrum of compound **6** (green trace) is also shown in Figure 5 and exhibits an almost identical absorption band at 330 nm.

The final product spectral band centered at 370 nm that is observed in Figure 5 is also identical to that of an authentic sample of **1** (blue trace), providing additional evidence that **1** is the final product. The corresponding NMR titration (Figure S3) shows that the hydrazine NH proton disappears immediately upon Cu(II) addition (fast hydrolysis of the hydrazine), while two new resonances appear at 5.78 and 6.74

dx.doi.org/10.1021/ic402723c | Inorg. Chem. 2014, 53, 2953−2962

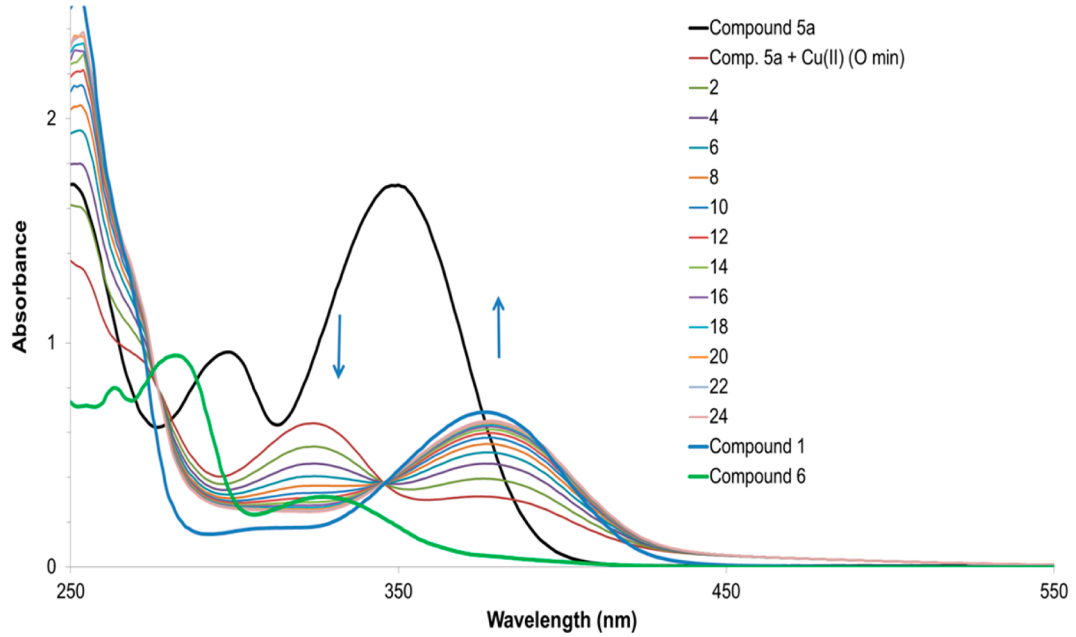

Figure 5. UV/vis spectral changes (recorded every 2 min) upon the addition of 1 equiv of Cu(II) to 1.0×10^{-4} M **5a** in a 99:1 acetonitrile/water mixture.

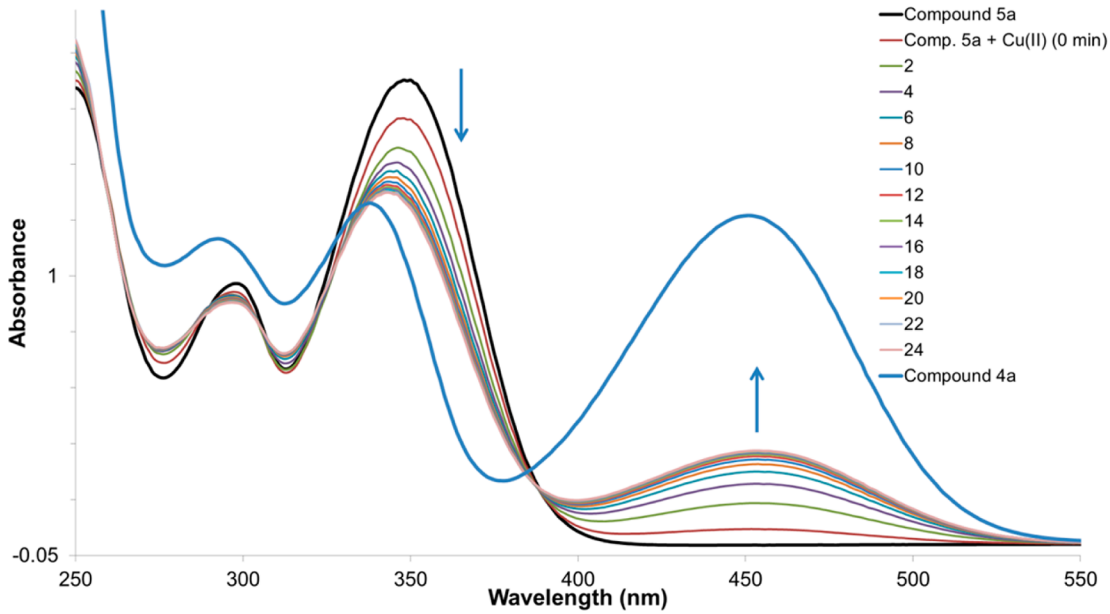

Figure 6. UV/vis spectral changes (recorded every 2 min) upon the addition of 1 equiv of Cu(II) to 1.0×10^{-4} M **5a** in a 90:10 acetonitrile/water mixture.

ppm that correspond to methine and aromatic resonances for intermediate **B** (Scheme 2), consistent with the **A** → **B** pathway. Addition of Cu(II) to the final product **1** does not produce any emission either, as we have previously reported.[22] ESI-MS experiments (Figure S4) also showed that **1** is the final product after addition of Cu(II) to **5a**, with the appearance of the sodiated peak at m/z 421 after several minutes. An additional peak at m/z 208 is present, likely corresponding to the hydrolyzed hydrazine associating with the copper cation, $[Cu(phenylhydrazine)(H_2O)_2]^+$ (m/z 208). MS−MS experiments on peaks of larger mass did not produce a peak at m/z 208 either, indicating that this peak is not due to simple fragmentation of larger species under these conditions.

Addition of Water. Of major significance is that upon addition of even larger amounts of water to the reaction medium, the spectroscopy completely changes when Cu(II) is added. Figure 6 shows the changes in the UV/vis spectrum when Cu(II) is added to a 90:10 acetonitrile/water mixture (compared with a 99:1 acetonitrile/water mixture; Figure 5). In this case, a broad peak at 460 nm slowly grows in with clean isosbestic points, instead of the 330 nm peak observed earlier under drier solvent conditions. The blue trace shows the absorption spectrum of compound **4a**, which has spectral features almost identical to what has slowly grown in, indicating that at higher water concentrations the reaction pathway radically changes. We propose that in this case, oxidation of the

dx.doi.org/10.1021/ic402723c | Inorg. Chem. 2014, 53, 2953−2962

Table 1. Hydrazine Hydrolysis and Alcohol Oxidation Rate Constants (min^{-1}) of 5a and 4a after Addition of 1 and 2 equiv of Cu(II) in Aqueous Acetonitrile Mixtures in Air

ACN/H_2O volume ratio	5a:Cu(II)	hydrolysis A → B	oxidation B → D (326 nm↓)	oxidation A → C (460 nm↑)	hydrolysis C → D (460 nm↓)	hydrolysis C → D (4a→ 1) (460 nm↓)
100:1	1:1	fast	0.061(4)			fast
	1:2	fast	fast			fast
99:1	1:1	fast	0.056(3)			fast
	1:2	fast	0.131(5)			fast
98:2	1:1	fast	0.024(3)			fast
	1:2	fast	0.022(3)			fast
95:5	1:1			0.63(10)	0.022(3)	0.096(10)
	1:2			0.71(1)	0.023(3)	0.099(10)
90:10	1:1			0.19(1)		0.039(5)
	1:2			0.24(4)		0.032(4)
50:50	1:1			0.012(2)		0.017(2)
	1:2			0.013(2)		0.013(1)

alcohol takes place first (**A** → **C**; Scheme 2) to yield hydrazone **4a**. Under these wet conditions, no fluorescence is observed; however, the same quinone product (**D**, compound **1**) is produced after the solution is allowed to sit overnight. Figure S5 shows the effect of adding metal cations to the unreduced hydrazone macrocycle **4a**. Almost instantaneous conversion of **4a** to compound **1** (black trace) occurs in the presence of Cu(II), indicating that Cu(II) can hydrolyze the unreduced hydrazone as well. The addition of Hg(II) and Fe(III) also produce hydrolysis, but the kinetics is slower. Similarly, no luminescence changes were observed for the reaction of **4a** with Cu(II). Addition of Cu(II) to **5a** in 90:10 acetonitrile/water also revealed radically different peaks in the mass spectrum (Figure S6) compared with what was previously observed in dry acetonitrile (Figure S4). Compound **1** is still produced, but there is no peak at m/z 208, indicating that the hydrazine is not hydrolyzed when significant water is present. Also, there is also a small peak at m/z 511, which is two mass units less than the starting sodiated **5a** peak (m/z 513). This suggests the presence of the oxidized intermediate **C** (Scheme 2). In MS–MS experiments, the peak at m/z 513 was shown not to produce the m/z 511 fragment.

Kinetics. We have shown qualitatively that altering the amount of water has a profound effect not only on the initial yellow- and green-emissive species when there is a relatively small amount of water in the solvent (Figure 4) but also on the relative rates of hydrolysis versus oxidation in this system when larger amounts of water are added (Figures 5 and 6). We have determined that the initial yellow fluorescence in very dry acetonitrile decays by first-order kinetics and is independent of the oxygen concentration. For N_2, O_2, and air-saturated solutions of **5a** + Cu(II), the initial yellow emission intensities are identical, and the decay rate constants are also approximately equal (1.20 ± 0.12 min^{-1}; Figure 4 left and Figure S7). The UV/vis changes under very dry conditions remain very similar to Figure 5 (Figure S8), indicating that the reaction proceeds through the same basic steps, and plotting the natural logarithm of the absorbance change versus time gives a straight line and a rate constant of 0.53 min^{-1} (Figure S9). In the presence of 0.25% water (~0.14 M), the disappearance of the green emission at band ~490 nm also follows first-order kinetics with a rate constant of ~1.5 min^{-1} in air (Figure 4 right and Figure S7). However, the initial emission intensity of the green fluorescence does depend on the concentration of dioxygen and was analyzed by separate Stern–Volmer investigations as discussed below.

Figure S10 shows a series of UV/vis spectra of **5a** with 2 equiv of added Cu(II) collected at different volume percentages of water in acetonitrile. Plotting the natural logarithm of the absorbance change versus time using the absorbance at 326 nm at low water concentration (Figure S11, following the decrease in spectral changes from Figure S10B, representing the **B** → **D** oxidation) or the absorbance at 460 nm at higher water concentration (Figure S12, following the increase in spectral changes from Figure S10E, representing the **A** → **C** oxidation) yields straight lines representing first-order kinetics, and the respective rate constants for these conversions are listed in Table 1.

At low water concentrations, hydrolysis of the hydrazine (**A** → **B**) is fast, and only oxidation of the alcohol (**B** → **D**) is observed, as previously explained. There is an apparent small decrease in the **B** → **D** oxidation rate as the water concentration increases, and it appears that the rates remain relatively constant at higher concentrations of Cu(II). At roughly 5% added water, oxidation of the alcohol (**A** → **C**) begins to compete with the hydrazine hydrolysis (**A** → **B**), as the peak at 460 nm is seen to grow in. For 1:2 **5a**/Cu(II) in the 95:5 acetonitrile/water mixture (Figure S10D), both the oxidation of **A** to **C** (growth of the peak at 460 nm) and the hydrolysis of **C** to **D** (subsequent decrease in the peak at 460 nm) are observed. At even higher concentrations of water, the conversion of **C** to **D** is not observable on this time scale, although conversion to **D** does take place over numerous hours. Oxidation of **A** to **C** appears to be more affected by the water concentration than the oxidation of **B** to **D**. Since intermediate **C** in Scheme 2 is identical to compound **4a**, the rate data for hydrolysis of the hydrazine by Cu(II) for **4a** were also determined (Figures S13 and S14). The rate decreases as before with the addition of more water, and the rates are approximately the same for the last two columns in the table and are both lower than the rate measured for the oxidation of **A** to **C**. We also tested the reaction of compound **6** with Cu(II); however, there was no change in the reaction, even after long periods of time, indicating that although intermediate **B** and compound **6** are isomers, they have very different oxidation potentials, as was previously reported.[24] We observed that the rates for both hydrolysis and oxidation decrease with added water, as shown in Table 1. Because of the poor solubility of **4a** in pure water, we synthesized compound **4c**

dx.doi.org/10.1021/ic402723c | Inorg. Chem. 2014, 53, 2953–2962

containing a carboxylic acid group that can form a carboxylate salt and is soluble in water. As expected, **4c** in the presence of Cu(II) in a 90:10 H_2O/acetonitrile mixture only very slowly converts to **1** over the course of several hours (Figure S15).

Cyclic Voltammetry. Cyclic voltammetry data for compounds **1**, **4a**, **5a**, and **6** were recorded using tetrabutylammonium perchlorate (TBAP) as the electrolyte and CH_2Cl_2 as the solvent (Figure S16). Whereas compound **1** shows two one-electron reductions at −1.07 and −1.51 V, which are characteristic of the individual carbonyl reductions of the unsymmetric 1,8-disubstituted anthraquinone,[27] compound **4a** shows only a single reversible one-electron reduction at −1.39 V and two irreversible oxidations at 0.95 and 1.63 V. We attribute the reversible peak to the reduction of the lone external carbonyl group in **4a** and the irreversible peaks to the hydrazine amine/imine oxidations. The reduction peak is missing for the reduced compound **5a** as no carbonyl is present, whereas the irreversible amine oxidation potentials were observed at similar potentials (0.93 and 1.40 V). Compound **6** shows one irreversible one-electron reduction peak for the external carbonyl group, and neither **5a** nor **6** have observable oxidation peaks for the alcohol groups.

Stoichiometry. The reaction is not catalytic [addition of 5% Cu(II) ion produces only a small change in the total concentration of **5a** after several hours], and increasing the copper concentration from 1 to 2 equiv does not appear to have a significant effect on the rate (Table 1). We do know that when the copper(II) salt with perchlorate (a noncoordinating anion) is used, crystalline $[Cu(CH_3CN)_4](ClO_4)$ is isolated from the reaction mixture.[28] To the best of our knowledge, the reaction of compound **5a** with Cu(II) (with noncoordinating anions) involves hydrolysis and oxidation to form **1** followed by slow oxidation of the hydrazine itself. Preliminary evidence from preparatory-scale reactions of Cu(II) with free phenylhydrazine or 2,4-dinitrophenylhydrazine in acetonitrile confirms that these hydrazines are oxidized, precipitating $[Cu(CH_3CN)_4]^+$ and forming other phenolic byproducts as determined by GC/MS (eq 1). This will be the subject of a separate paper.

$$\mathbf{5a} + \mathrm{Cu(II)} + \mathrm{O_2} \rightarrow \mathbf{1} + \mathrm{Cu(I)} + \text{phenolics} \quad (1)$$

This is not the case when the counteranion is chloride. Then the product recovered after reaction of **5a** with Cu(II) is **1**·$CuCl_2$, which can be isolated in crystalline form. Here the coordinating halogens reduce the oxidation potential of the copper metal center but still allow hydrolysis.

Role of Oxygen. We investigated the quenching behavior of oxygen for the green emission at 490 nm and determined that oxygen has both dynamic and static quenching components. When the solution is degassed with nitrogen prior to the addition of Cu(II), the green emission intensity increases over 10-fold compared with the intensity in air (Figure S17). Under pure oxygen conditions, the opposite occurs: the green emission intensity is significantly quenched and quickly decreases over time (Figure S18). Figure 7 shows upward curvature of a three-point Stern−Volmer plot of the steady-state green emission intensity (488 nm) versus dissolved oxygen concentration in acetonitrile under inert, air, and pure oxygen conditions. This curvature follows a quadratic relationship: $F_0/F = (1 + K_S[Q])(1 + K_D[Q])$, where F_0 is the fluorescence intensity in the absence of quencher and K_S and K_D are the static and dynamic quenching constants, respectively.[29] This indicates that both static quenching and dynamic quenching are involved. Lifetime data were also collected for the same reaction (Figure S19 and Table S2), and phase plane methods[30] and curve simulations[29] for a single exponential decay gave similar results. Plotting the lifetime data according to the expression $\tau_0/\tau = 1 + K_D[Q]$ produced the dynamic component alone, and the slope gave the value $K_D \approx 250\ M^{-1}$ (Figure 7). Substitution of K_D allowed the calculation of the static component as $K_S \approx 300\ M^{-1}$, which is of roughly equal magnitude to the dynamic quenching portion. Also, the bimolecular quenching constant (k_q) is given by the expression $K_D = k_q\tau_0$, from which the value $k_q = 1.2 \times 10^{10}\ M^{-1}\ s^{-1}$ is obtained, in excellent agreement with the diffusion-limited bimolecular quenching constant for dioxygen. The lifetime of the yellow emission at 560 nm was also determined to be short (2.6 ns) and independent of the water concentration (Figure S20 and Table S3).

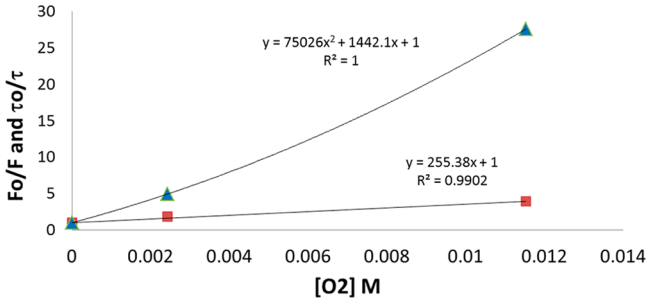

Figure 7. Stern−Volmer plot of 1×10^{-5} M **5a** with 2.0 equiv of added Cu(II) at 488 nm under pure N_2, air, and pure O_2 conditions. Triangles: steady-state F_0/F data. Squares: Lifetime data (τ_0/τ).

DISCUSSION

Corey and Knapp first reported Cu(II)-assisted hydrolysis of imines in the 1970s,[31] and Rezende and co-workers reported that chelated structures greatly enhance the rate of hydrolysis of imines by stabilizing the metal-associated transition state.[32] For **5a**, the polyether macrocycle that is positioned below the hydrazone is in an ideal position to chelate/coordinate the Cu(II) cation, including association with the imine nitrogen, which would increase the positive charge on the imine carbon though an inductive effect and promote attack by water on the imine carbon to yield the hydrolysis products. Only recently has hydrolysis of imines been employed in fluorescent chemodosimeters to monitor Cu(II) concentration, including our own previously reported work.[24,33]

Normally an increase in the amount of water would promote hydrolysis of imines; however the hydrolysis rate is also highly dependent on the hydration shell around the Cu(II) ion. We have observed that as very large amounts of water are added to the acetonitrile solvent, the rate-determining step switches from oxidation (**B** → **D**; i.e., hydrolysis of **A** to **B** is fast) to hydrolysis (**A** → **C**; hydrolysis is slowed). We expect that as more water is added, the equilibrium is shifted to a fully hydrated Cu(II) coordination sphere, preventing direct coordination with the hydrazone imine nitrogen and slowing the hydrolysis. From Table 1, the oxidation of the alcohol (**B** → **D**) is also kinetically slower than oxidation of the alcohol (**A** → **C**). Under dry conditions, this may be due to initial binding of the copper cation by macrocycle **5a**, promoting very rapid hydrolysis to produce intermediate **B**, which, because of the more electronegative carbonyl group, has a higher oxidation potential than **A**. We see this also from compound **6**, which is

dx.doi.org/10.1021/ic402723c | Inorg. Chem. 2014, 53, 2953−2962

resistant to oxidation by Cu(II) and dioxygen. Ultimately the different hydrolysis and oxidation rates under wet and dry conditions have value to synthetic chemists who wish to selectively oxidize or hydrolyze products with the same types of functional groups.

It is likely that the initial yellow emission observed when **5a** and Cu(II) are combined is due to the complexation of Cu(II) with **5a**, inducing an ICT photophysical change, as previously observed for these types of macrocycles.[22,23,25,26] The presence of slightly more water, which results in the sudden appearance of the green emission, may be due to simple differences in the coordination shell of the copper ion involving substitution of acetonitrile by water. Evidence to support this comes from the respective rate constants for the decay of the yellow and green emission intensities compared with the corresponding UV−vis changes under the same conditions. Both the yellow and green emission bands disappear at ∼20−30 times greater rates than the corresponding UV/vis kinetic changes, indicating that the fluorescence changes likely follow the rate of hydrazine hydrolysis while the UV/vis changes follow the oxidation of the alcohol (intermediate **B**) to the final product. From the Stern−Volmer fluorescence data, the static quenching observed is likely due to complexation of oxygen with a copper cation ligated in some fashion to the green-fluorescent intermediate, which is consistent with formation of a metal complex promoting luminescence in the first place. Site-specific damage of DNA by phenylhydrazine in the presence of Cu(II) presumably involves oxygen-derived active species (copper−oxygen complexes) implicated in the mechanism, similar to the results presented here.[34] Work to identify the phenylhydrazine byproducts is ongoing and will be reported elsewhere.

■ CONCLUSION

We have demonstrated that selective imination of the internal carbonyl of **1** occurs upon the addition of hydrazines, as opposed to imination at the external carbonyl as previously observed with ketamine formation involving transition-metal-catalyzed imination. The resulting phenylhydrazone produces a selective chemodosimeter (irreversible) sensitive only to Cu(II), proceeding though two intense fluorescence intermediates that are themselves water-dependent. Decomposition of hydrazones via two distinct pathways in the presence of Cu(II)/O_2 is also dependent on larger water content, which leads ultimately to the same product. This chemistry has consequences for synthetic applications, depending on whether hydrolysis or oxidation is the desired outcome. Under dry conditions, the hydrazone is initially cleaved, followed by oxidation of the alcohol. Under wet conditions, the opposite occurs. Of particular interest is that the intermediate green emission under dry conditions has both dynamic and static quenching components with dioxygen. The static quenching component suggests that the green-fluorescent intermediate involves complexation of dioxygen with a copper metal center coordinated to the fluorescent macrocycle involved in the slow oxidation of the secondary alcohol.

■ EXPERIMENTAL SECTION

General Procedures. Elemental analyses were conducted using an Exeter CE-440 elemental analyzer. Elemental analysis results are reported for samples and copper perchlorate previously dried in an Abderhalden flask at 100 °C to minimize the moisture content. ^{1}H NMR spectra (200 MHz) were obtained at room temperature in $CDCl_3$. Infrared spectra were obtained using a Bruker Alpha spectrophotometer. Absorbance data were collected using an HP 8452A diode array spectrophotometer or a Varian Cary 50 spectrometer. Emission studies were conducted using a SPEX Fluoromax fluorimeter. Mass spectrometry was conducted using a Varian 500-MS IT electrospray ionization (ESI) mass spectrometer. Cyclic voltammograms were recorded using a CH Instruments 660 electrochemical workstation. Melting points were determined using open capillaries and are uncorrected. The synthesis of **1** has previously been reported.[27] Copper(II) perchlorate trihydrate was purchased from Aldrich and used without further purification.

Synthesis of 1,8-Oxybis(ethyleneethoxyethyleneethoxy)-9-(phenylazo)-10-anthraquinone (4a). Phenylhydrazine (130 mg, 1.2 mmol) was suspended in 6 mL of methanol, and 0.4 mL of concentrated H_2SO_4 was added. To the resulting clear solution was added 1,8-oxybis(ethyleneethoxyethyleneethoxy)-9,10-anthraquinone (**1**) (100 mg, 0.25 mmol) dissolved in 5−10 mL of methanol. The resulting solution was stirred for 0.5 h and mixed with 100 mL of distilled water, affording an orange solid, which was filtered off, washed several times with distilled water, and air-dried. The compound was purified on a silica gel column using a 98:2 methylene chloride/methanol mixture. Yield: 100 mg (80%). Mp: 194−197 °C. Anal. Calcd for $C_{28}H_{28}N_2O_6$: C, 68.84; H, 5.78; N, 5.73%. Found: C, 68.86; H, 5.74; N, 5.68%. ^{1}H NMR ($CDCl_3$ at 25 °C): δ 3.06−4.40 (*m*, 16H, CH_2−O in polyether chain); 6.85−7.94 (m, 13H, ArH from anthraquinone + phenyl group); 9.02 (bs, 1H, NH). ^{13}C NMR ($CDCl_3$ at 25 °C): δ 69.28; 69.37; 69.72; 69.87; 69.98; 70.36; 70.53; 70.69; 114.02; 117.22; 117.96; 119.06; 120.92; 121.06; 127.80; 128.86; 129.89; 133.58; 134.75; 144.72; 153.58; 155.72; 184.78. IR: 1644 cm^{-1} (carbonyl); 3270 cm^{-1} (−NH−).

Synthesis of 1,8-Oxybis(ethyleneethoxyethyleneethoxy)-9-(2,4-dinitrophenylazo)-10-anthraquinone (4b). 2,4-Dinitrophenylhydrazine (238 mg, 1.2 mmol) was suspended in 6 mL of methanol and mixed with 0.4 mL of concentrated H_2SO_4. To the resulting clear solution was added **1** (100 mg, 0.25 mmol) dissolved in 5−10 mL of methanol. A red-orange solid precipitated immediately, and the mixture was cooled overnight and filtered. The solid was further purified on a silica gel column using a 98:2 methylene chloride/methanol mixture. Yield: 125 mg (85%). Mp: 218−220 °C. Anal. Calcd for $C_{28}H_{26}N_4O_{10}$: C, 58.13; H, 4.53; N, 9.68%. Found: C, 58.21; H, 4.49; N, 9.59%. ^{1}H NMR ($CDCl_3$ at 25 °C): δ 3.26−4.49 (m, 16H, CH_2−O in polyether chain); 7.19−7.91 (m, 8H, ArH from anthraquinone + DNP); 9.08 (bs, 1H, NH); 11.55 (s, 1H, ArH from DNP). ^{13}C NMR ($CDCl_3$ at 25 °C): δ 68.03; 68.74; 69.10; 69.35; 69.53; 69.65; 70.61; 70.68; 109.73; 115.99; 117.44; 117.65; 119.41; 120.45; 123.02; 129.26; 129.74; 130.48; 132.01; 134.06; 134.83; 138.32; 144.66; 153.75; 155.49. IR: 1674 cm^{-1} (carbonyl); 3310 cm^{-1} (−NH−).

Synthesis of 1,8-Oxybis(ethyleneethoxyethyleneethoxy)-9-(4-carboxylphenylazo)-10-anthraquinone (4c). In a round-bottom flask, 15 mL of water and 5 mL of concentrated H_2SO_4 were added, followed by 4-hydrazinobenzoic acid (0.478 g, 3.14 mmol). The solution was heated to 65 °C and stirred for 15−20 min to give a clear solution. **1** (0.500 g, 1.26 mmol) was added at the same temperature, and the solution was stirred for 10 min, after which the temperature was increased to 90 °C. This temperature was maintained for 12 h, followed by suction filtration of the hot solution and washing of the solid with hot water (2 × 50 mL). The product was dried and purified by recrystallization from hot acetonitrile. Yield: 0.350 g (52%). Mp: 247−249 °C. Anal. Calcd for $C_{29}H_{27}N_2NaO_8$: C, 62.81; H, 4.91; N, 5.05%. Found: C, 62.26; H, 5.39; N, 5.09%. ESI-MS: calcd for protonated **4c** 533.56, found 533.3; calcd for sodiated **4c** 555.5, found 555.3. ^{1}H NMR ($CDCl_3$ at 25 °C): δ 3.14−3.22 (m, 1H, CH_2−O, polyether); 3.29−3.49 (m, 5H, CH_2−O, polyether); 3.63−3.69 (m, 2H, CH_2−O in polyether chain); 3.77−4.65 (m, 8H, CH_2 −O in polyether chain);7.37−7.52 (m, 5H, ArH from anthraquinone + phenyl ring); 7.63−7.71 (m, 2H, ArH from anthraquinone); 7.78−7.83 (m, 1H, ArH from phenyl ring); 7.94−7.97 (d, 2H, ArH from anthraquinone); 9.61 (s, 1H, NH). IR: 1648 cm^{-1} (carbonyl); 3243 cm^{-1}(−NH−).

dx.doi.org/10.1021/ic402723c | Inorg. Chem. 2014, 53, 2953−2962

Synthesis of 1,8-Oxybis(ethyleneethoxyethyleneethoxy)-9-(phenylazo)-10-hydroxyanthrone (5a). *Method A.* **4a** (200 mg, 0.41 mmol) was suspended in 20 mL of 95% ethanol and mixed with $NaBH_4$ (0.016 g, 0.41 mmol). The solution was stirred for 2 h, mixed with 100 mL of distilled water, and extracted with 50 mL of methylene chloride. The methylene chloride solution was dried with anhydrous sodium sulfate and filtered, and most of the solvents were evaporated under reduced pressure. Diethyl ether was diffused into the methylene chloride solution, yielding a cream-colored solid.

Method B. **4a** (200 mg, 0.41 mmol) was suspended in 20 mL of THF under a N_2 atmoshphere and mixed with $LiAlH_4$ (0.016 g, 0.41 mmol). The solution was stirred for 3 h, slowly mixed with 100 mL of saturated ammonium chloride solution, and extracted with 50 mL of methylene chloride. The methylene chloride solution was dried with anhydrous sodium sulfate and filtered, and most of the solvents were evaporated under reduced pressure. Diethyl ether was diffused into the methylene chloride solution, yielding a cream-colored solid.

Melting point and spectroscopic characterization revealed that both methods yielded **5a**. Yield: 150 mg (70%). Mp: 145−148 °C. Anal. Calcd for $C_{28}H_{30}N_2O_6$: C, 68.59; H, 6.11; N, 5.71%. Found: C, 68.35; H, 6.15; N, 5.48%. ESI-MS: calcd for protonated **5a** 491.28, found 491.30. ^{1}H NMR ($[CD_3]_2SO$ at 25 °C): δ 3.08−4.35 (m, 16H, CH_2−O in polyether chain); 5.29−5.33 (d, 1H, anthrone); 5.75 (s, 2H, solvated CH_2Cl_2); 6.35−6.39 (d, 1H, OH); 6.72−7.41 (m, 11H, ArH from anthraquinone + phenyl group); 9.01 (bs, 1H, NH). IR: 3313 cm^{-1} (−NH−), 3372 cm^{-1} (−OH). No carbonyl stretching was observed.

Crystallography. X-ray-quality crystals were obtained by diffusing diethyl ether into methylene chloride/methanol solutions. Crystallographic data were collected at 293 K (**4b**) or 100 K (**5a**) using Mo Kα radiation. Cell constants were determined after integration from typically more than 9000 reflections.[35] Structures were solved by direct methods using SIR97[36] and refined using SHELXL-97.[37] Data reduction and refinement were completed using the WinGX suite of crystallographic software.[38] All non-hydrogen atoms were refined with anisotropic displacement parameters, and all hydrogen atoms were placed in ideal positions and refined as riding atoms with relative isotropic displacement parameters, with the exception of hydrogen-bonded protons, which were found from the difference map. Table S1 in the Supporting Information lists additional crystallographic and refinement information.

The space group $P21/c$ did provide a solution for **4b**; however, the disorder of the anthraquinone macrocycle could not be satisfactorily modeled to produce a reasonable R value. The space group Pc resulted in two different macrocycles within the asymmetric unit with different ring conformations, which were modestly restrained using five C−O and C−C DFIX instructions, yielding a satisfactory result. Low-temperature data for **4b** improved the thermal parameters but left higher R values for both the $P21/c$ and Pc solutions. An absolute configuration for this chiral molecule could not be determined. Three neighboring anthraquinone carbon atoms in the structure of **5a** were essentially two-dimensional and were refined as isotropic only.

■ ASSOCIATED CONTENT

Supporting Information

NMR, MS, and crystallographic characterization data and kinetic, cyclic voltammetric, and spectroscopic data. This material is available free of charge via the Internet at http://pubs.acs.org.

■ AUTHOR INFORMATION

Corresponding Author

*E-mail: asykes@usd.edu.

Notes

The authors declare no competing financial interest.

■ ACKNOWLEDGMENTS

The authors thank NSF-EPSCOR (EPS-0554609) and the South Dakota Governor's 2010 Initiative for financial support and the purchase of a Bruker SMART APEX II CCD diffractometer. We also thank Aravind Baride and Dr. P. Stanley May at the University of South Dakota for nanosecond lifetime measurements.

■ REFERENCES

(1) Domaille, D. W.; Que, E. L.; Chang, C. J. *Nat. Chem. Biol.* **2008**, *4*, 168.
(2) Barceloux, D. G.; Barceloux, D. *Clin. Toxicol.* **1999**, *37*, 217.
(3) (a) Que, E. L.; Domaille, D. W.; Chang, C. J. *Chem. Rev.* **2008**, *108*, 1517. (b) Gaggelli, E.; Kozlowski, H.; Valensin, D.; Valensin, G. *Chem. Rev.* **2006**, *106*, 1995.
(4) Flemming, C.; Trevors, J. *Water, Air, Soil Pollut.* **1989**, *44*, 143.
(5) Chu, L.; Liu, D.; Wang, Y.; Li, Y.; Liu, H. *Chin. J. Appl. Ecol.* **2004**, *15*, 119.
(6) Schultheis, A. S.; Sanchez, M.; Hendricks, A. C. *Hydrobiologia* **1997**, *346*, 85.
(7) EPA National Primary Drinking Water Regulations. http://water.epa.gov/drink/contaminants/index.cfm#1 (accessed Dec 4, 2012).
(8) Quang, D. T.; Kim, J. S. *Chem. Rev.* **2010**, *110*, 6280.
(9) Valeur, B. *Molecular Fluorescence: Principles and Applications*; Wiley-VCH: Weinheim, Germany, 2001.
(10) (a) Chen, C.; Wang, R.; Guo, L.; Fu, N.; Dong, H.; Yuan, Y. *Org. Lett.* **2011**, *13*, 1162. (b) Wang, H. H.; Xue, L.; Fang, Z. J.; Li, G. P.; Jiang, H. *New J. Chem.* **2010**, *34*, 1239. (c) Zhao, Y.; Zhang, X. B.; Han, Z. X.; Qiao, L.; Li, C. Y.; Jian, L. X.; Shen, G. L.; Yu, R. Q. *Anal. Chem.* **2009**, *81*, 7022. (d) Ajayakumar, G.; Sreenath, K.; Gopidas, K. R. *Dalton Trans.* **2009**, 1180. (e) Zheng, Y.; Gattás-Asfura, K. M.; Konka, V.; Leblanc, R. M. *Chem. Commun.* **2002**, 2350. (f) De Santis, G.; Fabbrizzi, L.; Licchelli, M.; Mangano, C.; Sacchi, D.; Sardone, N. *Inorg. Chim. Acta* **1997**, *257*, 69. (g) Corradini, R.; Dossena, A.; Galaverna, G.; Marchelli, R.; Panagia, A.; Sartor, G. *J. Org. Chem.* **1997**, *62*, 6283.
(11) (a) Hennrich, G.; Walther, W.; Resch-Genger, U.; Sonnenschein, H. *Inorg. Chem.* **2001**, *40*, 641. (b) Martínez, R.; Zapata, F.; Caballero, A.; Espinosa, A.; Tárraga, A.; Molina, P. *Org. Lett.* **2006**, *8*, 3235.
(12) (a) He, G.; Zhang, X.; He, C.; Zhao, X.; Duan, C. *Tetrahedron* **2010**, *66*, 9762. (b) Zhou, Y.; Wang, F.; Kim, Y.; Kim, S. J.; Yoon, J. *Org. Lett.* **2009**, *11*, 4442. (c) Kim, Y. R.; Kim, H. J.; Kim, J. S.; Kim, H. *Adv. Mater.* **2008**, *20*, 4428. (d) Lee, M. H.; Kim, H. J.; Yoon, S.; Park, N.; Kim, J. S. *Org. Lett.* **2008**, *10*, 213. (e) Xiang, Y.; Tong, A.; Jin, P.; Ju, Y. *Org. Lett.* **2006**, *8*, 2863.
(13) (a) Zhang, Y. J.; He, X. P.; Hu, M.; Li, Z.; Shi, X. X.; Chen, G. R. *Dyes Pigm.* **2011**, *88*, 391. (b) Wen, Z.-C.; Yang, R.; He, H.; Jiang, Y.-B. *Chem. Commun.* **2006**, 106. (c) Singh, A.; Yao, Q.; Tong, L.; Still, W. C.; Sames, D. *Tetrahedron Lett.* **2000**, *41*, 9601. (d) Ambrosi, G.; Ciattini, S.; Formica, M.; Fusi, V.; Giorgi, L.; Macedi, E.; Micheloni, M.; Paoli, P.; Rossi, P.; Zappia, G. *Chem. Commun.* **2009**, 7039. (e) Amendola, V.; Bergamaschi, G.; Buttafava, A.; Fabbrizzi, L.; Monzani, E. *J. Am. Chem. Soc.* **2010**, *132*, 147.
(14) Zhou, Z.; Fahrni, C. J. *J. Am. Chem. Soc.* **2004**, *126*, 8862.
(15) Lu, D.; Lei, J.; Tian, Z.; Wang, L.; Zhang, J. *Dyes Pigm.* **2012**, *94*, 239.
(16) Basa, P. N.; Bhowmick, A.; Schulz, M. M.; Sykes, A. G. *J. Org. Chem.* **2011**, *76*, 7866.
(17) Basa, P. N.; Bhowmick, A.; Medicine Horn, L.; Sykes, A. G. *Org. Lett.* **2012**, *14*, 2698.
(18) (a) Xu, Z.; Baek, K. H.; Kim, H. N.; Cui, J.; Qian, X.; Spring, D. R.; Shin, I.; Yoon, J. *J. Am. Chem. Soc.* **2010**, *132*, 601. (b) Wang, Q.; Xie, Y.; Ding, Y.; Li, X.; Zhu, W. *Chem. Commun.* **2010**, *46*, 3669. (c) Shao, J.; Yu, X.; Lin, H.; Lin, H. *J. Mol. Recognit.* **2008**, *21*, 425.
(19) Allen, J. R.; Cynkowski, T.; Desai, J.; Bachas, L. G. *Electroanalysis* **1992**, *4*, 533.

(20) Kaneda, T.; Umeda, S.; Ishizaki, Y.; Kuo, H. S.; Misumi, S.; Kai, Y.; Kanehia, N.; Kasai, N. *J. Am. Chem. Soc.* **1989**, *111*, 1881.
(21) Kadarkaraisamy, M.; Caple, G.; Gorden, A. R.; Squire, M. A.; Sykes, A. G. *Inorg. Chem.* **2008**, *47*, 11644.
(22) Kadarkaraisamy, M.; Sykes, A. G. *Inorg. Chem.* **2006**, *45*, 779.
(23) Kadarkaraisamy, M.; Sykes, A. G. *Polyhedron* **2007**, *26*, 1323.
(24) Basa, P. N.; Sykes, A. G. *J. Org. Chem.* **2012**, *77*, 8428.
(25) Young, V. G., Jr.; Quiring, H. L.; Sykes, A. G. *J. Am. Chem. Soc.* **1997**, *119*, 12477.
(26) *Chemosensors: Principles, Strategies, and Applications*; Wang, B., Anslyn, E. V., Eds.; John Wiley & Sons: Hoboken, NJ, 2011.
(27) Delgado, M.; Gustowski, D. A.; Yoo, H. K.; Gatto, V. J.; Gokel, G. W.; Echegoyen, L. *J. Am. Chem. Soc.* **1988**, *110*, 119.
(28) Csoregh, I.; Kierkegaard, P.; Norrestam, R. *Acta Crystallogr.* **1975**, *B31*, 314.
(29) Lakowicz, J. R. *Principles of Fluorescence Spectroscopy*, 3rd ed.; Springer Scientific: New York, 2006; p 277.
(30) Adamson, A. W.; Demas, J. N. *J. Phys. Chem.* **1971**, *75*, 2463.
(31) Corey, E. J.; Knapp, S. *Tetrahedron Lett.* **1976**, *17*, 3667.
(32) Machado, V. G.; Nascimento, M. G.; Rezende, M. C. *J. Braz. Chem. Soc.* **1993**, *4*, 76.
(33) Kim, M. H.; Jang, H. H.; Yi, S.; Chang, S. K.; Han, M. S. *Chem. Commun.* **2009**, 4838.
(34) Yamamoto, K.; Kawanishi, S. *Chem. Res. Toxicol.* **1992**, *5*, 440.
(35) *SAINT*, version 6.1; Bruker Analytical X-ray Systems: Madison, WI, 1999.
(36) Altomare, A.; Burla, M. C.; Camalli, M.; Cascarano, G. L.; Giacovazzo, C.; Guagliardi, A.; Moliterni, A. G. G.; Polidori, G.; Spagna, R. *J. Appl. Crystallogr.* **1999**, *32*, 115.
(37) Sheldrick, G. M. *SHELX97: Programs for Crystal Structure Analysis*, release 97-2; Universität Göttingen: Göttingen, Germany, 1998.
(38) Farrugia, L. J. *J. Appl. Crystallogr.* **1999**, *32*, 837.